High efficiency, broadband solar cell architectures based on arrays of volumetrically distributed narrowband photovoltaic fibers

Brendan O'Connor,[1] Denis Nothern,[2] Kevin P. Pipe,[1,3] and Max Shtein[2,4]

[1]*Department of Mechanical Engineering, University of Michigan, Ann Arbor, Michigan 48109, USA*
[2]*Department of Materials Science and Engineering, University of Michigan, Ann Arbor, Michigan 48109, USA*
[3]*pipe@umich.edu*
[4]*mshtein@umich.edu*

Abstract: We propose a novel solar cell architecture consisting of multiple fiber-based photovoltaic (PV) cells. Each PV fiber element is designed to maximize the power conversion efficiency within a narrow band of the incident solar spectrum, while reflecting other spectral components through the use of optical microcavity effects and distributed Bragg reflector (DBR) coatings. Combining PV fibers with complementary absorption and reflection characteristics into volume-filling arrays enables spectrally tuned modules having an effective dispersion element intrinsic to the architecture, resulting in high external quantum efficiency over the incident spectrum. While this new reflective tandem architecture is not limited to one particular material system, here we apply the concept to organic PV (OPV) cells that use a metal-organic-metal-dielectric layer structure, and calculate the expected performance of such arrays. Using realistic material properties for organic absorbers, transport layers, metallic electrodes, and DBR coatings, 17% power conversion efficiency can be reached.

OCIS codes: (350.0350) Other area of optics; (350.6050) Solar Energy.

References and links

1. W. Shockley, and H. J. Queisser, "Detailed balance limit of efficiency of p-n junction solar cells," J. Appl. Phys. **32**(3), 510–519 (1961).
2. M. A. Green, "Third generation photovoltaics: ultra-high conversion efficiency at low cost," Prog. Photovoltaics **9**(2), 123–135 (2001).
3. S. B. Rim, S. Zhao, S. R. Scully, M. D. McGehee, and P. Peumans, "An effective light trapping configuration for thin-film solar cells," Appl. Phys. Lett. **91**(24), 243501 (2007).
4. K. Tvingstedt, V. Andersson, F. Zhang, and O. Inganas, "Folded reflective tandem polymer solar cells doubles efficiency," Appl. Phys. Lett. **91**(12), 123514 (2007).
5. J. Y. Kim, K. Lee, N. E. Coates, D. Moses, T. Q. Nguyen, M. Dante, and A. J. Heeger, "Efficient tandem polymer solar cells fabricated by all-solution processing," Science **317**(5835), 222–225 (2007).
6. A. Hadipour, B. de Boer, J. Wildeman, F. B. Kooistra, J. C. Hummelen, M. G. R. Turbiez, M. M. Wienk, R. A. J. Janssen, and P. W. M. Blom, "Solution-processed organic tandem solar cells," Adv. Funct. Mater. **16**(14), 1897–1903 (2006).
7. P. Peumans, A. Yakimov, and S. R. Forrest, "Small molecular weight organic thin-film photodetectors and solar cells," J. Appl. Phys. **93**(7), 3693–3723 (2003).
8. L. A. A. Pettersson, L. S. Roman, and O. Inganas, "Modeling photocurrent action spectra of photovoltaic devices based on organic thin films," J. Appl. Phys. **86**(1), 487–496 (1999).
9. H. Kuraseko, T. Nakamura, S. Toda, H. Koaizawa, H. Jia, and M. Kondo, "Development of flexible fiber-type poly-Si solar cell," Conference Record of the 2006 IEEE 4th World Conference on Photovoltaic Energy Conversion, **Vols. 1–2** 1380–1383 (2006).
10. B. O'Connor, K. P. Pipe, and M. Shtein, "Fiber based organic photovoltaic devices," Appl. Phys. Lett. **92**(19), 193306 (2008).
11. M. R. Lee, R. D. Eckert, K. Forberich, G. Dennler, C. J. Brabec, and R. A. Gaudiana, "Solar power wires based on organic photovoltaic materials," Science **324**(5924), 232–235 (2009).
12. X. Fan, Z. Z. Chu, F. Z. Wang, C. Zhang, L. Chen, Y. W. Tang, and D. C. Zou, "Wire-shaped flexible dye-sensitized solar cells," Adv. Mater. **20**(3), 592–595 (2008).

#127867 - $15.00 USD Received 6 May 2010; revised 17 Jun 2010; accepted 18 Aug 2010; published 7 Sep 2010

13. C. Kim, and J. Kim, "Organic photovoltaic cell in lateral-tandem configuration employing continuously-tuned microcavity sub-cells," Opt. Express **16**(24), 19987–19994 (2008).
14. B. O'Connor, K. H. An, K. P. Pipe, Y. Zhao, and M. Shtein, "Enhanced optical field intensity distribution in organic photovoltaic devices using external coatings," Appl. Phys. Lett. **89**(23), 233502 (2006).
15. M. Agrawal, and P. Peumans, "Broadband optical absorption enhancement through coherent light trapping in thin-film photovoltaic cells," Opt. Express **16**(8), 5385–5396 (2008).
16. H. Hoppe, and N. S. Sariciftci, "Organic solar cells: An overview," J. Mater. Res. **19**(7), 1924–1945 (2004).
17. M. M. Wienk, M. P. Struijk, and R. A. J. Janssen, "Low band gap polymer bulk heterojunction solar cells," Chem. Phys. Lett. **422**(4-6), 488–491 (2006).
18. F. Yang, R. R. Lunt, and S. R. Forrest, "Simultaneous heterojunction organic solar cells with broad spectral sensitivity," Appl. Phys. Lett. **92**(5), 053310 (2008).
19. E. Palik, Handbook of Optical Constants of Solids (Academic Press; 1st edition, 1985).
20. B. O'Connor, C. Haughn, K. H. An, K. P. Pipe, and M. Shtein, "Transparent and conductive electrodes based on unpatterned, thin metal films," Appl. Phys. Lett. **93**(22), 223304 (2008).
21. G. Dennler, K. Forberich, M. C. Scharber, C. J. Brabec, I. Tomis, K. Hingerl, and T. Fromherz, "Angle dependence of external and internal quantum efficiencies in bulk-heterojunction organic solar cells," J. Appl. Phys. **102**(5), 054516 (2007).
22. A. Meyer, and H. Ade, "The effect of angle of incidence on the optical field distribution within thin film organic solar cells," J. Appl. Phys. **106**(11), 113101 (2009).
23. I. G. Hill, A. Kahn, Z. G. Soos, and R. A. Pascal, "Chem. "Charge-separation energy in films of pi-conjugated organic molecules," Chem. Phys. Lett. **327**(3-4), 181–188 (2000).
24. M. C. Scharber, D. Mühlbacher, M. Koppe, P. Denk, C. Waldauf, A. J. Heeger, and C. J. Brabec, "Design rules for donors in bulk-heterojunction solar cells – Towards 10% energy-conversion efficiency," Adv. Mater. **18**(6), 789–794 (2006).
25. The MatchWorks, Inc., Matlab R2009a (2009).
26. F. J. López-Hernández, R. Pérez-Jiménez, and A. Santamaría, "Ray-tracing algorithms for fast calculation of the channel impulse response on diffuse IR wireless indoor channels," Opt. Eng. **39**, 2775–2780 (2000).
27. H. A. Macleod, Thin-film Optical Filters, 3rd Ed. (Taylor & Francis, 2001).
28. H. Hoppe, N. Arnold, N. S. Sariciftci, and D. Meissner, "Modeling the optical absorption within conjugated polymer/fullerene-based bulk-heterojunction organic solar cells," Sol. Energy Mater. Sol. Cells **80**(1), 105–113 (2003).
29. A. Premoli, and M. L. Rastello, "Minimax refining of wide-band antireflection coatings for wide angular incidence," Appl. Opt. **33**(10), 2018–2024 (1994).
30. D. P. Partlow, and T. W. O'Keeffe, "Thirty-seven layer optical filter from polymerized solgel solutions," Appl. Opt. **29**(10), 1526–1529 (1990).
31. K. M. Ho, C. T. Chan, C. M. Soukoulis, R. Biswas, and M. Sigalas, "Photonic band gaps in three dimensions: New layer-by-layer periodic structures," Solid State Commun. **89**(5), 413–416 (1994).
32. R. R. King, D. C. Law, K. M. Edmondson, C. M. Fetzer, G. S. Kinsey, H. Yoon, R. A. Sherif, and N. H. Karam, "40% efficient metamorphic GaInP/GaInAs/Ge multijunction solar cells," Appl. Phys. Lett. **90**(18), 183516 (2007).
33. G. D. Wei, S. Y. Wang, K. Renshaw, M. E. Thompson, and S. R. Forrest, "Solution-processed squaraine bulk heterojunction photovoltaic cells," ACS Nano **4**(4), 1927–1934 (2010).

1. Introduction: the fiber OPV tandem concept

Tandem solar cells combining absorbers with different bandgaps that cover complementary parts of the solar spectrum reduce thermalization losses and increase the cell voltage [1,2]. Organic tandem solar cells have been considered in two main configurations (shown schematically in Fig. 1a,b) – transmissive and reflective [3–6]. In the more common transmissive configuration, multiple sub-cells are stacked such that spectral components not absorbed by the front cell are potentially absorbed by the back cell(s). The sub-cells are typically connected in series, for example by placing a recombination electrode between them. In this configuration, the layer thicknesses and compositions are optimized via optical and transport modeling [7,8], subject to the restriction that the photocurrents from all sub-cells must be matched. This design has its origins in monolithic inorganic solar concentrator PV cells [32]. However, unlike inorganic concentrator cells, organic solar cells that are aimed at low cost will likely not employ solar tracking. This restriction can be a limiting factor in terrestrial applications, where a range of illumination angles and wavelengths can magnify resistive losses in a sub-cell. Alternatively, two sub-cells can be placed next to each other at an angle (forming a "V" profile), such that incident light that is not absorbed by one sub-cell is reflected onto and potentially captured by the apposing sub-cell. At very sharp V angles the incident light can be trapped

#127867 - $15.00 USD Received 6 May 2010; revised 17 Jun 2010; accepted 18 Aug 2010; published 7 Sep 2010

efficiently [3]. However, this design is limited to two complementary sub-cells, and the intensity distribution along the sub-cell length is highly uneven (particularly at sharp V angles). Due to typical variations in the open circuit voltage (V_{OC}) and fill factor (FF) of organic solar cells with illumination intensity [7], this latter effect potentially makes it difficult to achieve the optimal power point of the cell.

Here we propose a novel tandem solar cell architecture, illustrated schematically in Fig. 1(c), that is based on a collection of efficient narrow-band absorbing sub-cells whose cumulative response can be made efficient over a broad incident spectrum by engineering efficient reflection of off-resonance spectral components among the constituent sub-cells. Such an architecture can be realized in the form of arrays of fiber-shaped solar cells that are distributed throughout a volume. This arrangement can be achieved, for example, by 3-dimensional weaving and/or by embedding solar cell fibers in a clear polymer matrix. We describe the details of several promising arrangements and calculate their expected performance based on experimentally validated optical and transport models of organic solar cells and optical coatings. Realistic material combinations and geometries are predicted to yield performance significantly exceeding the state-of-the-art in organic PV cells.

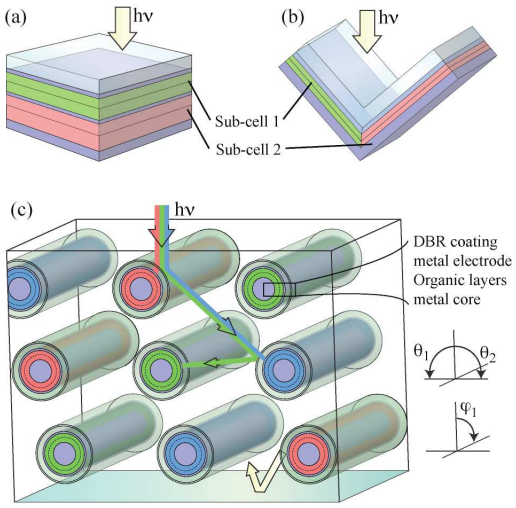

Fig. 1. Tandem solar cell designs including (a) a traditional transmissive solar cell design, (b) a reflective tandem solar cell in a V-shape configuration, and (c) an example of a reflective fiber based tandem cell design consisting of three rows of three spectrally-tuned photovoltaic sub-cells. The fiber OPV cells consist of a distributed Bragg reflector (DBR), a thick spacer layer, a transparent top electrode, the active organic layers, and finally an optically thick center electrode. Note that the fibers are not drawn to scale and are expected to be no less than 50 μm in diameter.

Below we first discuss general considerations for designing a volumetrically-distributed, internally-dispersive tandem solar cell using color-tuned fiber sub-cells. We then discuss the simulation framework used to model and optimize the performance of individual solar cells as well as fiber arrays. Using this framework, we first consider the performance of an array of fibers, which all have an identical cell structure optimized for absorption efficiency. To demonstrate the advantage of the tandem solar cell concept, we then consider the performance of an array comprised of color-tuned fibers, which incorporate narrow-band dielectric filters / reflectors, showing that the architecture can lead to high overall power conversion efficiency. Along with the simulation results, considerations for implementation are discussed in detail.

#127867 - $15.00 USD Received 6 May 2010; revised 17 Jun 2010; accepted 18 Aug 2010; published 7 Sep 2010

2. Design of a fiber OPV cell to be used in a volumetrically distributed reflective tandem

Several variants of fiber based-PV cells have been demonstrated, in particular by using organic semiconductors which can be easily deposited on non-planar substrates [9–12]. Here, we utilize a simple heterojunction OPV cell consisting of a metal-organic-metal layer sequence that is deposited onto a fiber (Fig. 2b) rather than a planar (Fig. 2a) substrate [10]. Light enters the device from the outside, opposite the substrate, unlike traditional OPV cells in which light enters the device through the substrate (e.g. indium tin oxide coated glass). The motivation for using a metal-organic-metal layer structure instead of a traditional configuration employing ITO is two-fold: a) eliminating ITO potentially improves manufacturability, reliability and cost-effectiveness, and b) it allows for a stronger optical microcavity that can be tuned to efficiently absorb light over a narrower part of the spectrum [13–15]. The latter consideration will be important in the overall design of the new tandem architecture.

The individual OPV cells considered here (Fig. 2e) consist of a semitransparent silver cathode, an optical spacer (working simultaneously as a charge transport layer), an active absorbing layer, another optical spacer which doubles as an exciton blocking layer, an optically thick silver electrode, and finally the fiber substrate (listed in the order of each layer's position in the path of incident light). Numerous commercially available organic dye molecules can be identified to cover a 200 nm or greater band of the incident spectrum with a high coefficient of absorption (i.e. $>1.5\text{x}10^5$ cm^{-1}) within a 300–1000 nm spectral range [7,16–18]. Thus, for simplicity we assume a generic material for the absorber layer capable of absorbing over a 200 nm optical bandwidth between 300 and 1000 nm. The real part of the refractive index of the absorber is set to $n = 1.75$, and the extinction coefficient is set to $k = \lambda\alpha/4\pi$ over the 200 nm absorption band and $k = 0$ at all other wavelengths, where λ is the wavelength of light and the absorption coefficient, $\eta = 1.5\text{x}10^5$ cm^{-1}. A nominal exciton diffusion length (L_D) of 20 nm is also assumed for this layer [7]. The refractive index of the remainder of the cell includes 1.75 for the optical spacers and a wavelength-dependent value for silver taken from literature [19]. The thickness of the semitransparent top electrode is set to 10 nm, and the thickness of the back electrode is set to 100 nm. A 10 nm Ag film has been shown to have a sheet resistance comparable to ITO making it a suitable alternative as a transparent conducting electrode [20]. Finally, the thicknesses of the optical spacers and absorption layer are designed to maximize the short circuit current (j_{SC}) of the individual OPV cell and are given below for specific tandem designs.

3. Approach to modeling and optimization of individual fiber OPV cells and multi-fiber arrays

The design and analysis of the fiber OPV cells uses optoelectronic models presented and validated in detail elsewhere [7,20]. Briefly, the model allows us to quantify the optical field intensity distribution throughout the OPV cell using the transfer matrix approach [8]. From the optical field intensity distribution, the exciton generation rate is calculated, and the exciton diffusion equation is numerically solved to determine the external quantum efficiency (η_{EQE}). The boundary conditions for the diffusion equation are: 1) complete exciton dissociation at the boundary between the electron donor and acceptor layers (here, the absorber and front side optical spacer), and 2) zero exciton diffusion at the opposite boundary (i.e. absorber / back side optical spacer). Following exciton dissociation, 100% charge collection efficiency at the electrodes is assumed [7]. A qualitative view of a flat-band energy level structure for this cell configuration is given in Fig. 2e. The j_{SC} is then predicted by integrating the product of η_{EQE} and incident photon flux over the solar spectrum (AM1.5G, truncated between 300 and 1000 nm).

#127867 - $15.00 USD Received 6 May 2010; revised 17 Jun 2010; accepted 18 Aug 2010; published 7 Sep 2010

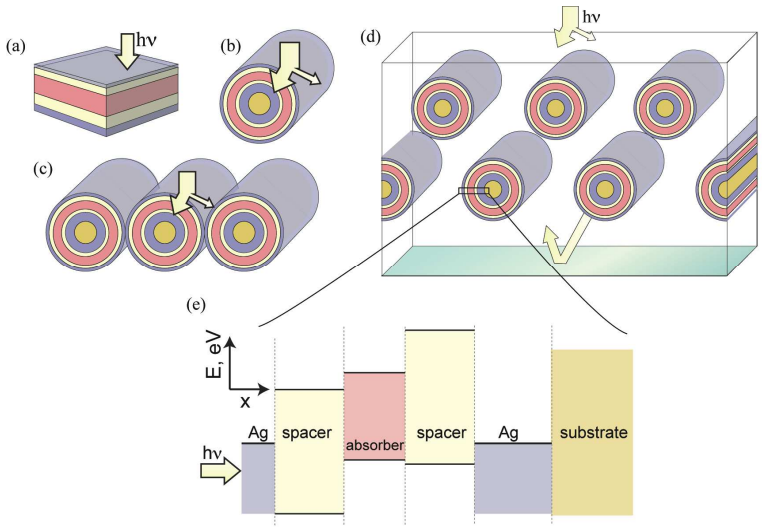

Fig. 2. Device structures modeled for a single solar cell design: (a) planar metal-organic-metal solar cell, (b) fiber OPV cell geometry, (c) row of fibers, and (d) matrix of fiber cells. (e) Qualitative view of the energy band structure for the solar cell in all configurations.

To model the OPV cell on a fiber substrate, we consider it to be a collection of vanishingly small planar cells tangentially distributed along the circumference of the fiber, each having light rays incident at an arbitrary angle throughout a 180-degree range. This approach has been used to accurately model organic solar cells in many studies, including those that consider the dependence on illumination angle [21,22]. Other key parameters of OPV cell performance include the fill factor (FF), and open circuit voltage (V_{OC}). The V_{OC} of each cell is set to be 0.4 V less than the potential given by the optical bandgap (roughly the HOMO-LUMO gap) of the absorbing material [13,23]. The FF is assumed to be 0.7, a value that is observed in high performance OPV cells [24].

To evaluate multi-fiber OPV systems, the model embodying an individual fiber OPV cell is combined with numerical ray-tracing. A multi-fiber unit cell is first constructed in which each fiber is assumed to be infinitely long. The location of each fiber within the unit cell is specified, and periodic boundary conditions are applied in the direction normal to the fiber axis, such that the array extends "horizontally". A line emitter, defined above the fiber system emits light rays towards the fiber bundle. A retro-reflector (with reflectivity = 1) is placed below the fiber bundle. In Fig. 3, a random sample of rays are traced for a two-row fiber OPV matrix [25]. In this simulation, rays incident on the left or right edge of the unit cell are translated to the opposite edge in order to satisfy the periodic boundary condition. On average the rays strike all surfaces of each fiber, suggesting that shading losses can be neglected [10]. This ray-tracing routine is carried out until the summed intensity of the rays remaining in the array is less than 0.5% of the input intensity. For the line emitter, 10,000 rays are generated (20,000 rays in the case of bundles with 20 rows of fiber cells) and randomly placed along the length of the emitter with even probability [26], resulting in a standard deviation of the predicted j_{SC} for repeated simulations of the larger bundles of less than 0.094 mA/cm^2 (based on the area occupied by the entire array – i.e. "real estate" of the module).

#127867 - $15.00 USD Received 6 May 2010; revised 17 Jun 2010; accepted 18 Aug 2010; published 7 Sep 2010

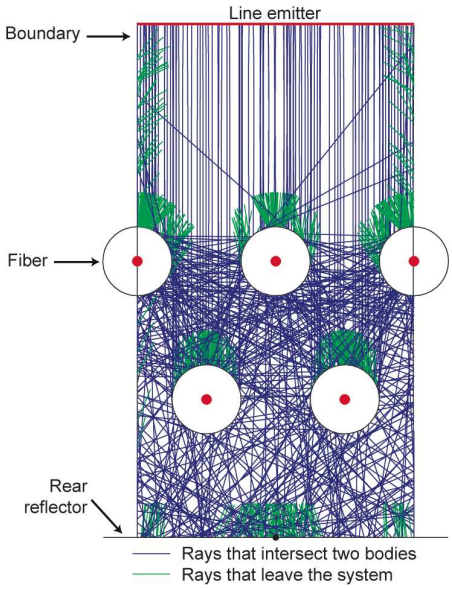

Fig. 3. Output of the ray-tracing program that is used to analyze periodic multi-fiber OPV systems. Sample rays are traced to visually inspect the performance of the bundled fiber OPV system. Rays that leave the system are shown in green, and rays from the emitter and those that are incident on at least two bodies are shown in blue.

A key aspect of the multi-fiber tandem design is that those incident wavelengths that are not efficiently harvested by a given fiber are efficiently reflected. An appropriately tuned metal-organic-metal cavity reflects a large portion of the off-resonant light. However, due to the large number of reflections experienced by a light ray on average, even a small amount of parasitic absorption in the outer electrode for a single pass can escalate to a substantial loss overall. Therefore, we further improve off-resonant reflectivity by applying dielectric coatings around the OPV fiber. A 30-layer dielectric coating is applied to the color-tuned OPV cells with an initial design based on multiple quarter wave stacks of 5-10 layers, forming a band pass filter. Each quarter wave stack gives rise to regions of high reflectivity near its characteristic wavelength; combining several such stacks forms regions of high reflectivity for spectral components that are off-resonance with the fiber cell's peak absorption. The initial coating configuration is refined by varying the individual layer thicknesses in an iterative process to maximize both transmission on-resonance and reflectivity off-resonance for a planar cell under normal illumination [15,27]. The coatings are applied around the fiber OPV cell on top of a thick (greater than 100 nm) transparent coating that reduces light coherence to minimize parasitic interference effects [28]. The coatings consist of two alternating materials having refractive indices of $n_H = 2.2$ and $n_L = 1.35$, these values being common in optical coating design [27]. For simplicity, the refractive indices of both the thick transparent (e.g. barrier) coating between the outer electrode and the DBR stack, as well as the clear matrix surrounding the coated fibers, are assumed to be the same as air (i.e. n = 1). This assumption is made based on the likelihood that the fiber array will be embedded in a clear polymer or glass matrix that has an index nearly identical to that of a typical barrier material (e.g. n = 1.4), leading to a conserved diffraction angle. Using n = 1 instead also conserves the diffraction angle but simplifies the model. An anti-reflection coating (ARC) at the surface of the clear matrix holding the fibers will minimize any differences associated with moving away from the n = 1 assumption. ARCs on glass have been designed with reflectivity below 1% over the visible spectrum and for a large range of incident angles [29]. In addition, while a host matrix with n = 1.4 would require a DBR redesign, this refractive index falls between the values for the

#127867 - $15.00 USD Received 6 May 2010; revised 17 Jun 2010; accepted 18 Aug 2010; published 7 Sep 2010

DBR coating materials, reducing the optical impedance and improving the coating's performance.

In the next two sections we apply this architecture and modeling approach to multi-fiber OPV cell arrays. We first consider the performance of arrays using only one OPV cell structure. Subsequently, multiple, spectrally tuned OPV cells are employed within the fiber matrix to maximize performance across the incident solar spectrum.

4. Design of multi-fiber OPV arrays

To investigate the performance of the volumetrically distributed, reflective tandem PV cell architecture, we begin by considering a single OPV cell in a planar configuration, then map its performance onto a single fiber; we then consider adjacent fibers, and finally multiple rows of fibers, as illustrated in Fig. 2.

Single-fiber architecture: We first examine an OPV cell with a single absorption layer capturing 500-700 nm light. Over this wavelength range, the power conversion efficiency is maximized by calculating the trade-off between current (limited by the solar photon flux density at each wavelength) and V_{OC} (defined as a constant that depends only on the chosen optical band gap of the absorption layer). Using the modeling described above, we find that the planar OPV cell structure resonant with the 500-700 nm band of incident light which maximizes j_{SC} consists of a 10 nm Ag electrode followed by a 52 nm optical spacer, 15 nm absorption layer, 52 nm exciton blocking layer, and finally a 100 nm Ag back contact. For this device, an optical bandpass filter is not yet applied. Under AM1.5G illumination, the OPV cell is predicted to have a short circuit current, j_{SC} = 8.2 mA/cm^2. Combining this with a FF = 0.7, and a V_{OC} determined to be 1.37 V results in a power conversion efficiency, η = 7.86%. Applying this structure to a fiber geometry results in a j_{SC} = 7.8 mA/cm^2; the reduction in j_{SC} relative to the planar analogue is due to increased reflection at oblique incident angles on the fiber surface. For comparison a planar OPV cell with a 200 nm ITO electrode with optimized layer thicknesses is predicted to have j_{SC} = 6.9 mA/cm^2 and η = 6.6%.

Planar array of fibers: To capture a portion of the reflected light, the fibers can be placed adjacent to one another, as might be encountered in a woven textile. A planar array of infinitely long fibers is illustrated in Fig. 2c; based on the ray-tracing model described above, this array is predicted to have a j_{SC} = 8.9 mA/cm^2, overcoming the losses associated with the fiber geometry under normal illumination, and outperforming the planar cell. (Note that in one aspect, the linear fiber array is similar to the V-shaped reflective tandem OPV cell discussed earlier.)

While a single row of fibers can increase the photocurrent substantially (~14% over a single fiber OPV cell, and 8.5% over a planar cell), much of the light initially reflected off the fiber surface is not trapped. In appropriately configured multi-row (3-dimensionally distributed) fiber OPV bundles decribed below, however, a majority of light rays that enter the fiber matrix bounce between the constituent fibers many times.

Volumetric array of fibers: We now consider multi-row fiber arrays, varying the depth from 1 to 20 rows. Due to improved packing, performance predicted by ray tracing models was generally best for fibers that were placed in a repeating "slant" arrangement (see Fig. 4) over that of a V- or W-shaped arrangement. For each set of rows, the distance between fibers in a slant arrangement was varied spatially both vertically and horizontally to maximize j_{SC}. The geometries of the best-performing bundles for 1, 2, 3 and 10 rows are shown in Fig. 4, with their calculated j_{SC} plotted in Fig. 5. For the 10-row system we observe a 36% improvement over the single fiber cell. As expected, there are diminishing returns with an increasing number of rows; at 10 rows, absorption of light over the wavelength range corresponding to the spectrum of the absorption layer exceeds 90%.

#127867 - $15.00 USD Received 6 May 2010; revised 17 Jun 2010; accepted 18 Aug 2010; published 7 Sep 2010

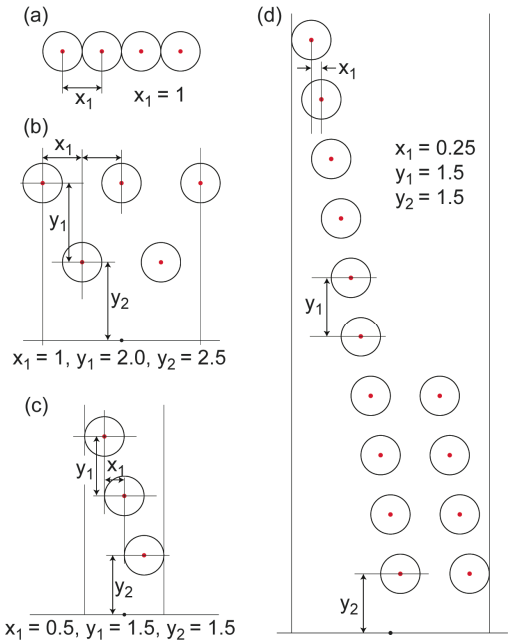

Fig. 4. (a-d) 2-dimensional coordinates for the best-performing fiber-OPV bundles for 1, 2, 3, and 10-row systems. These geometries are determined through a non-exhaustive search and further optimization is likely possible. The coordinates are given in units of fiber diameters.

Superimposed on the calculated photocurrent for fiber-based devices in Fig. 5 is the photocurrent of the widely studied planar heterojunction copper phthalocyanine (CuPc) - C_{60} cell having a thin semitransparent Ag metal electrode. The device structure consists of 10 nm Ag, 10 nm bathocuproine (BCP), 30 nm C_{60}, 25 nm CuPc, 8 nm MoO_3, and 100 nm Ag. The exciton diffusion length was set to 8 nm in CuPc and 20 nm in C_{60}, values in agreement with those measured in literature [20]. The device model used here has been shown to accurately predict the performance of this planar heterojunction PV cell [7,20]. Comparatively, this small-molecule OPV cell and the simplified cell initially described are similarly designed with metal electrodes and optical spacers sandwiching the absorption layer(s). The cavities in both cells are tuned for optimal photocurrent generation over a similar bandwidth, and with multiple fiber rows the incident light absorption is maximized. Consequently, the performance between the small molecule planar heterojunction and the simplified single cell design compare well, suggesting the simplified fiber design is a valid estimate of expected OPV performance.

5. Using multiple color-tuned fiber OPV cells to build an efficient broad-band array

Further increases in the efficiency of multi-fiber OPV cells can be realized by combining spectrally-tuned fiber devices in volumetric arrays. The individual OPV cells on fibers retain the same basic structure (i.e. metal-organic-metal), but the thicknesses of the absorber and other layers are modified to tune the optical microcavity and maximize the photocurrent of an individual fiber device over a specific spectral band [13]. Furthermore, a band-pass optical filter is added (as discussed in Section 3) to efficiently reflect off-resonant wavelengths while remaining transparent for on-resonance wavelengths. These coatings are uniquely designed for each type of spectrally tuned OPV-cell. The fiber arrays incorporate wavelength selective dispersion by virtue of their geometry and the DBR coating, such that incident light is effectively sorted among the sub-cells – a ray of particular wavelength bounces between the constituent fibers until it encounters (and is absorbed by) a complementary tuned fiber OPV cell.

#127867 - $15.00 USD Received 6 May 2010; revised 17 Jun 2010; accepted 18 Aug 2010; published 7 Sep 2010

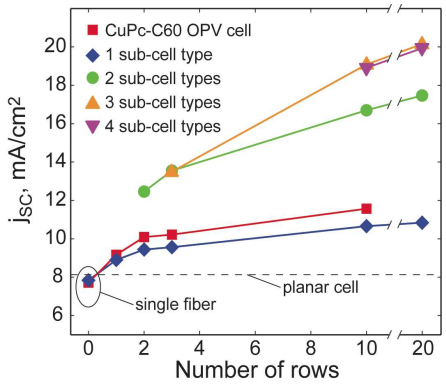

Fig. 5. (a) Predicted short circuit current for the fiber bundles ranging from a single fiber, to a fiber system consisting of 20 rows. Coordinates for the 1, 2, 3 and 10 row systems are given in Fig. 4. The number of sub-cells is varied from 1 to 4 designs with details of these designs provided in Table 1. Results for a similar OPV cell based on a planar heterojunction structure with CuPc and C_{60} as the donor-acceptor materials are shown for comparison.

Table 1. Optical absorption band, expected V_{OC}, and device structure of the fiber sub-cells used in the multi-fiber tandem OPV cells modeled in Fig. 4[a]

No.	Sub-cell	Absorption band, nm	V_{OC}, V	t_{Spacer}, nm	t_{Abs}, nm
1	i	500 – 700	1.37	52	15
2	i	450 – 650	1.51	44	15
	ii	650 – 850	1.06	72.5	10
3	i	350 – 550	1.86	31	12.5
	ii	550 - 750	1.25	55	12.5
	iii	750 - 950	0.91	87.5	10
4	i	300 - 500	2.08	25	15
	ii	365 - 665	1.47	45	15
	iii	630 - 830	1.09	70	12.5
	iv	800 - 1000	0.84	92.5	10

[a]The Number column indicates the number of sub-cells for the fiber bundles, the optical spacers above and below the absorption layer are set to the same thickness (t_{Spacer}) for design simplicity, and t_{Abs} is the thickness of the absorption layer.

The predicted j_{SC} of fiber bundles that combine 1, 2, 3, or 4 types of fibers (i.e. representing 1, 2, 3, or 4 complementary optical bands) is shown in Fig. 5, which also depicts the performance of arrays whose depths range from 1 to 20 rows of fibers. As previously mentioned, each fiber PV cell is optimized to have high efficiency over a 200 nm spectral band, with the target spectral band and layer thicknesses of the sub-cells for the range of fiber types provided in Table 1. The fiber spatial orientation is the same as the single cell designs (given in Fig. 4) while the color-tuned cell placement is varied within the fiber matrix to maximize performance. A complete optimization of color-tuned cell placement was not performed; however, the best performance was generally observed when the color-tuned cells were similar in number and evenly spaced. For the multi-color fiber systems, light trapping is slightly reduced due to the increased number of reflections before capture, yet there is a substantial gain in the spectral band of light capture. The color-tuned external quantum efficiency of the individual planar cells, along with the external quantum efficiencies of a 10-row, 4-color fiber system are given in Fig. 6a and Fig. 6b, respectively. The reflectivity of the sub-cell tuned between 630 and 830 nm is also provided as an example of performance typical for the filter-

#127867 - $15.00 USD Received 6 May 2010; revised 17 Jun 2010; accepted 18 Aug 2010; published 7 Sep 2010

OPV cell designs with high off-resonance reflectivity and high on-resonance absorption. Under the assumption that the absorber layer only absorbs over a 200 nm bandwidth, the microcavity OPV cells will inherently have a high degree of reflectivity off-resonance. However, the filters are important in mitigating the off-resonant parasitic absorption generally observed in the layers of the OPV cells.

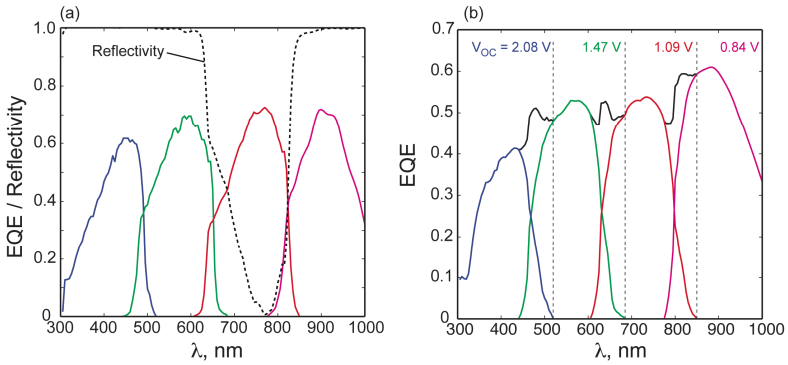

Fig. 6. Performance parameters for the 10-row, 4 color-tuned OPV fiber bundle. (a) External quantum efficiencies (EQEs) of the planar counterparts of the 4 microcavity tuned fiber OPV cells under normal illuminations. The reflectivity of one of the cells is also given to illustrate the high reflectivity for off-resonant wavelengths. (b) Total EQE along with the contributions of the separate color-tuned fibers in the 10-row, 4 color-tuned bundle. Predicted open circuit voltage is also given for each sub-cell.

The foregoing analysis predicts the array photocurrent. To predict the power conversion efficiency, we place the individual fiber cells in electrical series and/or parallel to match current and voltage and maximize power conversion efficiency. The vertical distribution of fibers will see varying intensity and thus each fiber in depth will have a unique maximum power point. However, we expect that the fiber with the same relative coordinate in adjacent unit cells will have the same current-voltage output. These cells can be added in parallel to sum the current without voltage losses. As the external wiring runs down the composite, when current is matched between the multi-cell parallel wiring, the circuit can be combined in series to sum voltage without current losses. This provides a means to sum power output from each fiber without significant losses. The open circuit voltage of each 4 sub-cell design is given in Fig. 6b, and as stated above the fill factor is assumed to be 0.7. Under these assumptions, the power conversion efficiency of the 4 color-tuned sub cell 10-row design is predicted to be 17.0%.

Performance at different angles of illumination: It is also important to consider the performance of these new reflective / inherently dispersive tandem architectures with illumination angle, as shown in Fig. 7. Here we examine the responsivity of a planar microcavity OPV cell tuned between 500 and 700 nm, and of a 2-row fiber bundle having the same type of OPV structure. It is observed that at low off-normal incident angles (relative to the plane of the fiber array), the reponsivity is similar; however, at very large incident angles the bundle system outperforms its planar counterpart. Also shown in Fig. 7 is the performance of the 10-row, 3-color tuned fiber OPV bundle. For this system, the specific symmetry of the "repeat unit" of the bundle results in a non-trivial dependence of efficiency on the 3-primary incident angle vectors. The results also indicate that while the 3-row bundle performance for a wide range of longitudinal incident angles (φ) is similar to that of the 2-row bundle, increasing the other incident angles results in a faster roll-off in efficiency. This highlights the importance of the interplay of illumination angle and array symmetry in the overall system design and optimization.

#127867 - $15.00 USD Received 6 May 2010; revised 17 Jun 2010; accepted 18 Aug 2010; published 7 Sep 2010

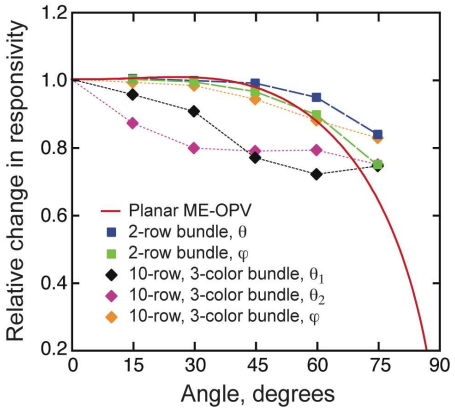

Fig. 7. The angular dependence of a planar metal-organic-metal OPV device and a 2-row fiber bundle having the same cell design. Also plotted is the performance of the 10-row, 3 color-tuned fiber bundle with the layout given in Fig. 4. The variation in the incident angle for the bundle is illustrated in Fig. 1c. The 10-row fiber bundle is asymmetric and the performance is therefore given for 3-angle variations. The relative responsivity is a measure of performance assuming the intensity on the top surface of the solar cell is constant with angle.

6. Considerations for implementation

Components of the proposed tandem architecture have been previously demonstrated. For example, individual fiber-based solar cells based on organic [10] and inorganic [9] materials have been reported. Methods exist to form DBR coatings on a variety of substrates by sputtering, thermal evaporation, solution coating, and other means [27,30]. Fabrication of 3-dimensional arrays of fiber- or rod-based solar cells could proceed by 3-D weaving, scaffolding [31], and monolithically embedding in transparent media. Bus-lines will be required to transport charge efficiently down long lengths of fiber. The bus-lines can be placed as metal strips underneath each fiber and will also act as light scattering sources. In the models, the fiber bundles are observed to be insensitive to exact fiber placement, such as vertical spacing between rows, suggesting that the implementation of bus-lines will not substantially alter device performance.

While the use of coated fiber bundles increases the total solar cell surface area and consequently the amount of organic, dielectric, and metal materials used beyond that of a planar cell occupying equivalent real estate, employing low-cost materials (e.g. organic absorbers and thin metal electrodes) can be effective. Furthermore, we anticipate the operational lifetime of the PV cells will be improved due to multiple levels of encapsulation (e.g. barrier coating, DBR stack, and clear matrix in which the fibers are embedded). We note, however, that the illumination intensity per surface area of the thin-film solar cell will be lower, potentially affecting device performance. A 1-row deep array of fibers has about 3 times more surface area than its planar counterpart of the same real estate. The 10-row deep fiber design of Fig. 5 has approximately 14 times more surface area. In a simple analysis, the surface of a given fiber sees 1/14-sun AM1.5 illumination intensity. For organic solar cells, the V_{OC} typically drops with illumination intensity while the FF often increases and the overall power conversion efficiency is not necessarily optimal at 1-sun [5,7,33]. How these parameters depend on illumination intensity depends substantially on the material and OPV cell design at hand, and in some instances optimal conversion efficiency occurs at low (e.g. less than 1/20th sun [33]) intensity. This suggests that the individual OPV cells can continue to perform efficiently, particularly when considering the wavelength distribution of light transmitted through the DBR coating. For example, for a 3-color tuned OPV cell bundle, the increase in surface area for the relevant spectral band is reduced by a factor of 3 relative to total active surface area. Taking this into

#127867 - $15.00 USD Received 6 May 2010; revised 17 Jun 2010; accepted 18 Aug 2010; published 7 Sep 2010

consideration, the 10-row bundle will see a reduced intensity per unit surface area of approximately 3/14 or 20% of an equivalent planar cell.

7. Summary and Outlook

An individual fiber OPV cell has been shown to be less efficient than its planar counterpart. However, simply placing multiple fibers adjacent to one another overcomes the losses through improved light trapping. Placing the fiber cells in a 3-dimensionally distributed bundle configuration leads to further enhancements in light trapping, resulting in an external quantum efficiency that approaches the internal quantum efficiency. By adding sub-cells that are tuned to efficiently convert light over a specific portion of the solar spectrum, the fiber system that efficiently traps light also acts as a built-in dispersion element, matching incident wavelengths of light to a complementary OPV cell. By virtue of optical microcavity design utilizing metallic electrodes and dielectric coatings, the opposing requirements of electrode transparency and conductivity can be decoupled to an extent. Here we have used a combination of optical and transport models to show that color-tuned OPV cells in a fiber matrix can lead to power conversion efficiencies over 17%, assuming modest absorption coefficients, metallic electrodes, and conservative assumptions regarding the fill factor. Through improved light trapping, broadband sensitivity, and output voltage optimization, this efficiency can be doubled over what is predicted for an optimized single junction cell having similar intrinsic properties. Additionally, improvements in the performance of single junction OPV cells will lead to improved performance of the fiber OPV tandem design. The full design space for this tandem architecture has not been exhausted in this study, and we expect that for color-tuned fiber OPV bundles a more complete and coupled optimization of cell design and fiber placement will lead to even further improvements in performance.

OPV device designs based on spatially distributed fibers offer several potentially powerful advantages over conventional planar devices. For example, electrical interconnections can be made with much greater latitude for current and voltage matching, in contrast to series-connected tandem cells. Furthermore, spatially distributed fibers can be placed into an inert matrix material that prevents the diffusion of oxygen and moisture, and offers considerable protection from mechanical damage.

Finally, the overall concept of a reflective, inherently dispersive tandem architecture involving volumetrically distributed sub-cells potentially can be applied to other sub-cell shapes and material systems, including inorganic PV cells, and/or combinations of organic and inorganic sub-cells.

Acknowledgments

We acknowledge the Air Force Office of Scientific Research (AFOSR) for their financial support of this work (grant no. FA9550-09-1-0109).

#127867 - $15.00 USD Received 6 May 2010; revised 17 Jun 2010; accepted 18 Aug 2010; published 7 Sep 2010